

# A Reticle Correction Technique to Minimize Lens Distortion Effects

Warren W. Flack, Gary E. Flores, Alan Walther and Manny Ferreira

Ultratech Stepper, Inc.

San Jose, CA 95134

Mix-and-match lithography is broadly accepted as a valuable strategy for reducing capital costs and increasing productivity in semiconductor manufacturing. The main technical challenge for mix-and-match lithography is to provide adequate overlay to support advanced device design rules. The overlay error consists of a number of components, including lens distortion of the various lithography tools. All optical lithography systems have a characteristic distortion signature which results from lens design and manufacturing. Lenses of a given design are usually matched during manufacturing to minimize the overlay effect of distortions in a multistepper environment. However, mix-and-match lithography frequently requires the use of systems of different field sizes from multiple vendors and technologies (1x, 5x, 4x). In this case, the lens distortion signatures can be very different between the lithography systems.

One approach to minimize the effect of lens distortion is to apply a series of corrections to the design database before reticle manufacturing. These corrections can be optimized to a specific lens or can be generic to remove the systematic errors of a class of lenses. This flexible approach offers the potential to remove lens distortion as a major factor in overlay error for mix-and-match lithography.

In this study, the distortion signature of an Ultratech 2244i lens was measured using an advanced registration measurement system. A correction for this distortion signature was applied to the design database and a mix-and-match test reticle fabricated. In order to quantify the effectiveness of this technique, a mix-and-match overlay study was performed using the same Ultratech 2244i and an advanced 5x reduction stepper. Overlay experiments were performed using both corrected and noncorrected reticles on the Ultratech system. An automated metrology system was used to collect overlay measurements distributed over the entire lens field area. Detailed analysis of the lens intrafield component of the overlay error using both reticles illustrates the advantages of applying reticle distortion corrections.

## 1.0 INTRODUCTION

Historically, global competition in integrated circuit fabrication has been based on both technological and economic factors. However, fabrication costs are now becoming the single dominant issue as the price of new high-volume production facilities approaches the billion dollar level [1]. Since lithography equipment represents a large fraction of this investment cost, it is also an excellent area in which to pursue cost savings. One technique that has been extremely successful in containing lithographic costs is mix-and-match lithography [1]. In this approach a less costly and higher throughput lithography tool is used for noncritical levels, while a higher resolution and more expensive lithography tool is only used on critical levels. The major technical challenge for mix-and-match lithography is to produce advanced technologies with the required device overlay.

To obtain maximum overlay performance when using multiple lithographic systems, each system must be calibrated or matched to the others [2]. Extensive analysis and modeling of overlay errors has been developed for system matching. These overlay errors can be divided into interfield and intrafield systematic sources. The interfield sources model the grid stage motion errors across the wafer while the intrafield sources model the overlay error within one field [3]. The intrafield model is described by equations for  $dX$  and  $dY$ :

$$dX(x,y) = T_{ix} + M_x x - \Theta_i y + \Psi_x xy + \Psi_y x^2 + D_3 x(x^2+y^2) + D_5 x(x^2+y^2)^2 \quad (1)$$

$$dY(x,y) = T_{iy} + M_y y + \Theta_i x + \Psi_y xy + \Psi_x y^2 + D_3 y(x^2+y^2) + D_5 y(x^2+y^2)^2 \quad (2)$$

where  $x$  and  $y$  are the coordinate location relative to the center of the field. The terms include die shift in  $x$  ( $T_{ix}$ ) and  $y$  ( $T_{iy}$ ), magnification in  $x$  ( $M_x$ ) and  $y$  ( $M_y$ ) and rotation ( $\Theta_i$ ), trapezoid in  $x$  ( $\Psi_x$ ) and  $y$  ( $\Psi_y$ ) third order ( $D_3$ ) and fifth order ( $D_5$ ). The terms that are dependant on the lens distortion of the various lithography tools include  $x$  and  $y$  magnification, rotation, third order and fifth order [4]. The lens dependant terms are an issue for mix-and-match lithography since the distortion signatures between various steppers can be very different. A study of non-concentric field matching has shown that the ideal lens for mix-and-match lithography should have as little distortion as possible relative to a reference grid [5]. Therefore it is not appropriate to simply match lenses relative to the distortions built into previous generation steppers.

One approach to minimize the effect of lens distortion is to apply a series of corrections to the design database before reticle manufacturing. This reticle correction technique has been used in the manufacturing of x-ray lithography masks to minimize the effects of high stress processing steps such as electroplating [6]. The intrafield overlay was corrected for rotation, magnification and non-orthogonality by changing the magnetic deflection of the e-beam. Vector plots of the field distortion residuals were significantly improved in comparison to the field distortion obtained before calibration [6]. In another study,  $x$  and  $y$  magnification corrections were applied during the

e-beam exposure of x-ray masks. These corrected masks were used on an x-ray stepper for mix-and-match lithography with an optical lithography tool [7].

The application of reticle corrections can also be used to remove lens distortions for mix-and-match lithography between two optical steppers. In this scenario, distortion corrected reticles could be created for either or both lithography systems. In practice, only the higher throughput lithography system would be adjusted since this is the noncritical lithography tool. This approach could be extended such that the reticle corrections applied to the noncritical system could be designed to actually match the distortion signature of the critical system for maximum mix-and-match correction.

## 2.0 RETICLE CORRECTIONS

In this study, an Ultratech 2244i 1x stepper was used as the high throughput, mix-and-match lithography system. The lens distortion for the 2244i system was determined using an indirect measurement technique [8]. A “master” test reticle covering the full 22 by 44 millimeters (mm) field is used as the design reference. This reticle contains a matrix of 23 by 13 test locations that were previously measured using a Leitz LMS 2020 position metrology system. This master test reticle was used to optically expose a “working” reticle using the 2244i stepper selected for lens characterization. After patterning and etching, the “working” reticle was then measured using the same position metrology system. The working reticle data can then be referenced to the master test reticle. The difference between measurements represents the lens distortion of the optical lens system in the 2244i. Note that this technique inherently contains measurement errors from the Leitz system [9]. The distortion vector plot of the 2244i lens system used in this study is shown in figure 1. The three sigma distortion values in  $x$  and  $y$  are 52 nanometers (nm) and 97 nm respectively.

This distortion data was used as the basis to manufacture a reticle that corrects for the 2244i lens distortion. There are numerous approaches that could be used to actually implement the reticle corrections. A preferred approach is to divide the reticle data into a large number of “cells” and locally correct the data using distortion vector data for each individual cell. Unfortunately, with currently installed e-beam systems, this approach requires significant computer resources, which would make the reticle cost prohibitive. Another approach is to fit the distortion data to a grid error model that can be corrected in the e-beam job deck commands. Standard grid error corrections are easy to implement, but have the disadvantage of leaving a residual of noncorrected error which reduces the effectiveness of the reticle correction technique. This is the approach used by Puisto [6] and Yanof [7] to manufacture x-ray photomasks. Because of its significant cost advantages, this is also the approach that was selected for this study.

Standard interfield or grid error models have been created for wafer overlay characterization [10]. A widely accepted grid error model for metrology analysis is described by equations for  $E_x$  and  $E_y$  [11]:

$$E_x(X,Y) = T_x + S_x X - \Theta_x Y \quad (3)$$

$$E_y(X,Y) = T_y + S_y Y + \Theta_y X \quad (4)$$

where  $X$  and  $Y$  are the coordinate locations (mm) in the reticle field. The error sources include translation error (nm) in  $X$  ( $T_x$ ) and  $Y$  ( $T_y$ ), scale magnification (ppm) in  $X$  ( $S_x$ ) and  $Y$  ( $S_y$ ) and field rotation (ppm) in  $X$  ( $\Theta_x$ ) and  $Y$  ( $\Theta_y$ ). Note that this model does not directly include orthogonality ( $\Phi$ ) as an error source. However, orthogonality (ppm) simply corresponds to the difference in field rotation terms ( $\Theta_y - \Theta_x$ ).

An analysis of variance (ANOVA) for the full field lens distortion from figure 1 produced the grid model results displayed in table 1. Orthogonality was calculated and is shown for the convenience of the reader. The goodness of fit (R squared) for the model is 0.0932 in  $x$  and 0.507 in  $y$ . Relative to an ideal fit of 1.0, this value indicates that there is a poor fit to the data in the  $x$  axis. However, an F test shows that the model is statistically significant at  $P < 0.05$  in both axis. The residual errors after applying this model to the lens distortion are shown in figure 2. The three sigma values in  $x$  and  $y$  are 49 nm and 67 nm respectively. This represents an improvement over the uncorrected data of 4% and 31% in  $x$  and  $y$  respectively. However, the overall residuals are still quite large, which suggests that a full field analysis is not the best approach to correcting this distortion data.

Upon close examination of the lens distortion data, it is apparent that the right and left sides of the 2244i field exhibit different patterns. Since the mix-and-match test reticle described in the experimental methods section consists of two identical 22 by 22 mm die, it would be easy to implement independent grid corrections for the right and left die. Therefore, the ANOVA was recalculated for the right and left sides separately to produce the two grid models displayed in table 2. The R squared values show that the left side of the field fits the grid model better than the right side. An F test shows that the model is statistically significant at  $P < 0.05$  for the left side only. The residual errors after applying these models to the lens distortion are shown in figure 3. The three sigma values in  $x$  and  $y$  are 45 nm and 42 nm respectively for the complete field. This represents an improvement over the uncorrected data of 12% and 57% in  $x$  and  $y$  respectively.

The concept of dividing the field into subfields for grid correction analysis could be extended to achieve even greater correction of the lens distortion. However, utilization of a large number of subfields suffers from complexity in the statistical analysis and the e-beam job deck creation. In addition, subfields that are a different size than individual die could create field butting errors inside of the die. Therefore, the grid analysis was stopped at two subfields for this study. A corrected test reticle was written using a MEBES III electron beam exposure system at a 0.1 micron address. The MEBES system accepts grid corrections for  $X$  and  $Y$  translation,  $X$  and  $Y$  alpha (scale) and orthogonality. The scale and orthogonality terms in table 2 were converted from ppm to nm by multiplying the subfield extent of 22 mm. The corrections used on the reticle are

shown in figure 4. The maximum corrections in  $x$  and  $y$  were 22.6 nm and 83.9 nm respectively. It is interesting to compare this figure with the lens distortions in figure 1. It is apparent that the applied corrections more closely match the left side of the lens distortions. This is consistent with the F test results obtained from the ANOVA.

### 3.0 EXPERIMENTAL METHODS

In order to evaluate the test reticle described in the previous section, a mix-and-match lithography test was performed using an Ultratech Stepper model 2244i (high throughput stepper) and a Canon model FPA 2500i2 (high resolution stepper). The Ultratech Stepper model 2244i is based on the 1x Wynne-Dyson Hershel lens design applied to i-line lithography with a field size of 22 x 44 mm square. Also incorporating i-line optics, the Canon FPA 2500i2 stepper provides a field size of 22 x 22 mm. Hence this allows two fields from the Canon stepper to be positioned within a single 22 x 44 mm field on the Ultratech 2244i.

A characterization reticle set for both steppers was used to provide the necessary grid and intrafield overlay measurements. The field layout for this set consisted of overlay and blindstep metrology patterns located within the field as shown in figure 5. A standard box-in-frame measurement structure is positioned at each overlay location for subsequent automated measurement, where the Canon stepper defines the outer frame structure and the Ultratech stepper defines the corresponding inner box structure as shown in figure 6. This design provides a total of 49 overlay locations per Canon field arranged in a periodic array of 7 rows by 7 columns extending to the 22 x 22 mm field boundary. Two versions of the Ultratech test reticle field were prepared. The first was a standard, noncorrected field. The second field contained the distortion corrections applied for translation, alpha and orthogonality as described in the previous section. Both the standard noncorrected field and the distortion corrected field were fabricated on the same reticle to minimize effects of noise from the e-beam system.

Wafers from the backend segment of a submicron CMOS process were utilized in this project. First, the Canon stepper patterned the reference grid on a metallized substrate film. The metal film was etched to transfer the reference level including alignment targets for the Ultratech 2244i. Next, both TEOS and nitride films were deposited over the patterned metal to simulate the process film stacks encountered at a dielectric reticle level. Alignment of the dielectric reticle to the metal level was then performed using the Ultratech 2244i. A cross sectional view of the entire composite film stack is shown in figure 7.

Four eight inch wafers were evaluated. Two were patterned using the distortion corrected reticle field and the other two were patterned using a standard reticle with no corrections. Each contained a total of 48 Canon fields or 24 2244i fields as shown in figure 8. A one-micron film of UCB-JSR ix500EL photoresist was coated and prebaked for 60 seconds at 90 °C prior to exposure. After

exposing, the wafers were post exposure baked for 60 seconds at 120°C and then developed for 60 seconds in PPD-523 (NMD-3 Metal Ion Free) developer for later overlay measurement.

Overlay was measured on a KLA 5700 Coherence Probe Microscope using 66 box-in-frame structures spread across the Ultratech field as shown in figure 5. A total of 14 Ultratech fields or 28 Canon fields were measured on each wafer at the locations designated by a ☆ in figure 8. With 24 narrow fields per wafer and 33 locations per field, 924 overlay measurements were collected per wafer. This field sampling strategy, which covers the full extent of the wafer, provides sufficient statistical degrees of freedom for extraction of grid parameters in the mix-and-match application. Also, when examining the pooled uncorrected mix-and-match error prior to modeling all corrections, a sample size of 924 provides a reasonable confidence interval for typical metrics such as the standard deviation and mean.

The KLA 5700 uses coherence probe technology to measure overlay [12]. Characterization was performed on the system to assure that the error due to the tool was negligible. Multiple measurements were taken on the overlay targets during the tool setup to determine the tool variance. Ten measurements on the overlay targets displayed a 3 sigma of 7 nm. Additionally, the Tool Induced Shift (TIS) has been characterized and seen to be less than 10 nm for layers up to 15 microns thick.

## 4.0 RESULTS AND DISCUSSIONS

After using the KLA 5700 to measure the resulting mix-and-match overlay error from the two groups of wafers, the data was analyzed on the KLAUT 2500 workstation to remove systematic grid errors from the data set. Reticle rotation due to the Ultratech 2244i was also removed from the data set. The removal of these terms is essential for this analysis to prevent other overlay error components from obscuring the residual interfield lens matching behavior.

The resulting mix-and-match overlay error for the noncorrected and corrected fields illustrated distinctly different characteristics. A summary of the  $x$  and  $y$  overlay errors for the corrected and noncorrected fields is shown in table 3. The corrected field shows an improvement of 30% in both the  $x$  and  $y$  standard deviations compared to the noncorrected case. This corresponds to a reduction of 19 nm and 14 nm for the  $x$  and  $y$  standard deviation. These improvements compare favorably with the calculated reductions in reticle correction section of 12% and 57% in  $x$  and  $y$  respectively.

Histograms showing the distributions of the  $x$  and  $y$  mix-and-match overlay errors for both the corrected and noncorrected reticles are shown in figures 9 and 10 respectively. It is interesting to note that all the distributions were statistically determined to be normal. This is to be expected for the corrected reticle since the systematic component of the lens distortion signature was removed. The distributions for  $x$  on the corrected versus the noncorrected reticle clearly illustrate a distinct improvement with a tighter distribution for the corrected case.

The difference between the experimentally determined mix-and-match errors and the calculated distortion reductions is probably due to several error sources in this study. The first is that all of the reticles that were manufactured contain grid errors from the MEBES III system. A second source is the measurement errors from the Leitz LMS 2020 create errors in the actual determination of the 2244i lens distortion. A third source is the measurement errors from the KLA 5700 which introduce errors in the determination of the mix-and-match overlay data. While none of these error sources are large, together they can easily account for the observed discrepancies.

The reticle corrections in this study were only applied to the Ultratech Stepper lens. There is no reason that this approach could not be extended to the high resolution stepper to further improve the mix-and-match overlay. This could be done by correcting the reticle on the high resolution stepper or making further corrections on the Ultratech reticle to match the lens distortions of high resolution stepper.

The implementation of grid distortion corrections using a small number of subfields has a minimal impact on reticle cost. However, the cost increase must be balanced against the final overlay improvement. In practice, it is anticipated that distortion corrected reticles would only be used on a few levels in a process that require more critical overlay.

## 5.0 CONCLUSIONS

A reticle correction technique to minimize lens distortion effects has been applied to mix-and-match of a large field high throughput stepper and a reduction stepper. The lens distortion signature of the Ultratech 2244i was optimized to a standard grid using corrections based on dividing the field into two subfields. A test reticle was fabricated containing both a corrected and noncorrected Ultratech 2244i field. Detailed intrafield overlay measurements of a mix-and-match lithography test using both the corrected and noncorrected field illustrated distinctly different matching behavior. The corrected reticle field shows an improvement of 30% in both the  $x$  and  $y$  standard deviations compared to the noncorrected field. This corresponds to a reduction of 19 nm and 14 nm for the  $x$  and  $y$  standard deviation. These improvements compare favorably with the calculated reductions in reticle correction section of 12% and 57% in  $x$  and  $y$  respectively.

## 6.0 ACKNOWLEDGMENTS

We would like to recognize the contributions of James Justen, Doug Vandenbroeke and Terry Lampe of Hoya Micro Mask in the fabrication of the reticles used in this study.

## 7.0 REFERENCES

1. J. Maltabes, M. Hakey, A. Levine, "Cost/Benefit Analysis of Mix-and-Match Lithography for Production of Half-Micron Devices", *Optical/Laser Lithography VI Proceedings*, SPIE **1927** (1993).
2. A. Yost and W. Wu, "Lens Matching and Distortion in a Multistepper, Submicron Environment", *Integrated Circuit Metrology, Inspection and Process Control III Proceedings*, SPIE **1087** (1989).
3. W. Flack, G. Flores, J. Pellegrini and M. Merrill, "An Optimized Registration Model for 2:1 Stepper Field Matching", *Optical/Laser Microlithography VII Proceedings*, SPIE **2197** (1994).
4. J. Armitage, "Analysis of Overlay Distortion Patterns", *Integrated Circuit Metrology, Inspection and Process Control II Proceedings*, SPIE **921** (1988).
5. M. Preil, T. Manchester, A. Minvielle, R. Chung, "Minimization of Total Overlay Errors when Matching Non-Concentric Exposure Fields", *Optical/Laser Microlithography VII Proceedings*, SPIE **2197** (1994).
6. D. Puisto, "Electron-beam Lithography Optimization for 0.25  $\mu\text{m}$  X-ray Mask Making", *Photomask Technology and Management Proceedings*, SPIE **2087** (1993).
7. A. Yanof et. al., "Overlay Measurement and Analysis of X-ray/Optical Lithography for Mix-and-Match Device Applications", *Electron-Beam, X-Ray, and Ion Beam Submicrometer Lithographies for Manufacturing IV Proceedings*, SPIE **2194** (1994).
8. S. Hwang, B. Ruff, "Optimizing Distortion For a Large Field Submicron Lens", *Optical/Laser Microlithography VII Proceedings*, SPIE **2197** (1994).
9. L. Land, J. Whittey, "Environmental Effects on Registration and Accuracy Data on Quartz Photomasks Utilizing the LMS 2000 - Laser Metrology System", *Integrated Circuit Metrology, Inspection and Process Control IV*, SPIE **1261** (1990).
10. M. van den Brink, C. de Mol and R. George, "Matching Performance for Multiple Wafer Steppers Using an Advanced Metrology Procedure", *Integrated Circuit Metrology, Inspection and Process Control II Proceedings*, SPIE **921** (1988).
11. KLASS III<sup>®</sup> Reference Manual, Appendix Models and Algorithms.
12. M. Davidson et. al., "First Results of a Product Utilizing Coherence Probe Imaging for Wafer Inspection", *Integrated Circuit Metrology, Inspection and Process Control II Proceedings*, SPIE Vol. 921 (1988).

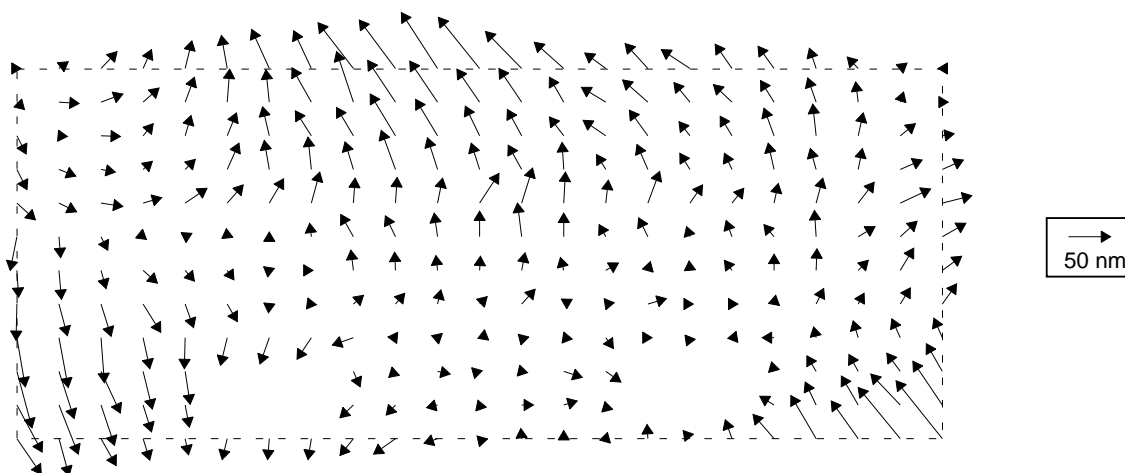


Figure 1: 2244i Lens distortion plot with no correction applied.

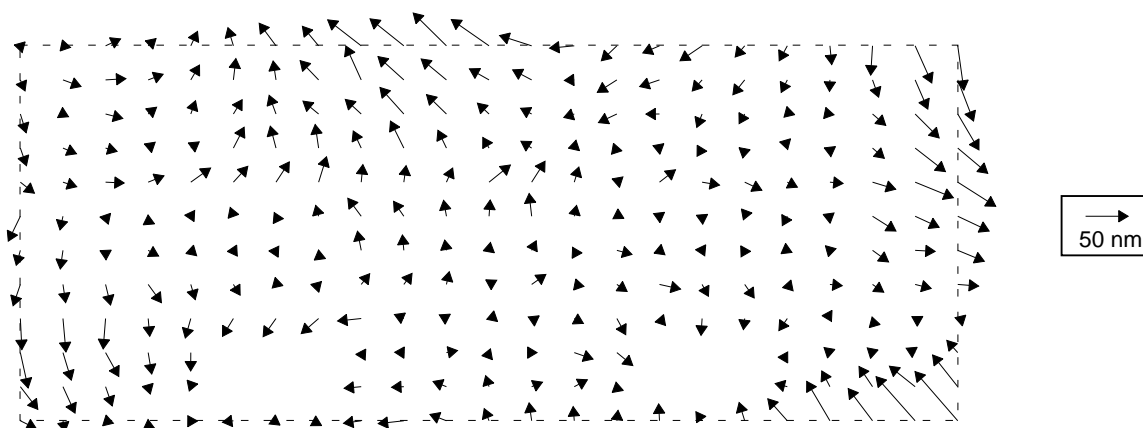


Figure 2: Residual plot of lens distortion after full field correction.

Full Field Model	X Error	Y Error
Translation (nm)	2.832	11.982
Scale (ppm)	-0.6835	-4.657
Rotation (ppm)	-0.6706	2.508
Orthogonality (ppm)	3.179	
Model R squared	0.0932	0.5074
Model Prob > F	0.0000	0.0000

Table 1: Analysis of Variance for full field lens distortion.

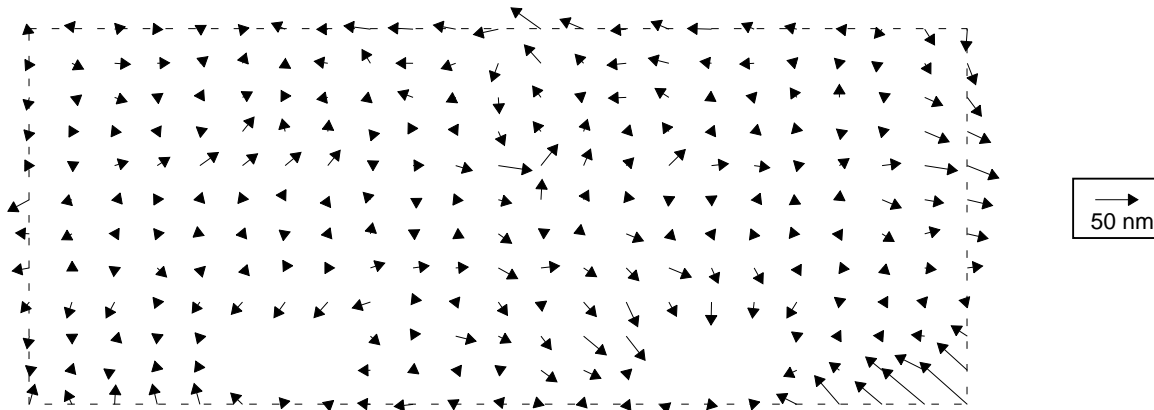


Figure 3: Residual plot of lens distortion after independent right and left side correction.

Right/Left Model	Left X Error	Left Y Error	Right X Error	Right Y Error
Translation (nm)	14.59	9.027	-14.53	13.83
Scaling (ppm)	-2.957	-8.175	0.4830	-0.6737
Rotation (ppm)	-0.9112	6.921	-0.3205	0.8156
Orthogonality (ppm)	7.832		1.136	
Model R squared	0.4730	0.9092	0.0126	0.0402
Model Prob> F	0.0000	0.0000	0.4597	0.0803

Table 2: Analysis of Variance for independent right and left field lens distortion.

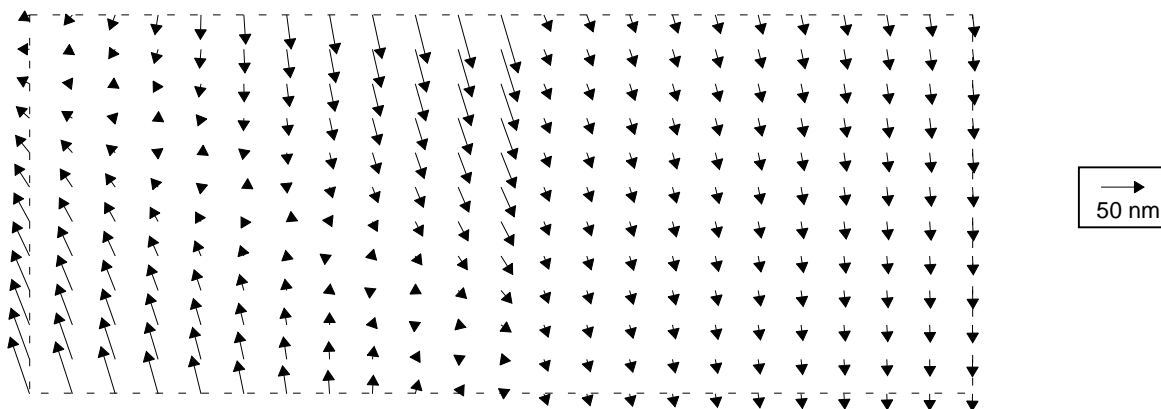


Figure 4: Plot of the corrections applied to the test reticle.

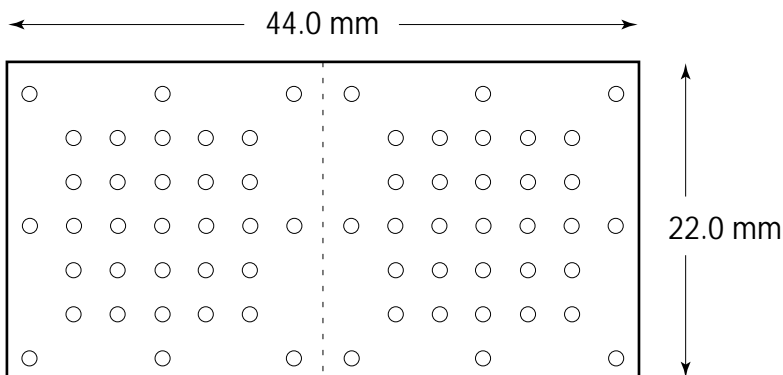


Figure 5: Field layout for Ultratech reticle showing overlay metrology locations.

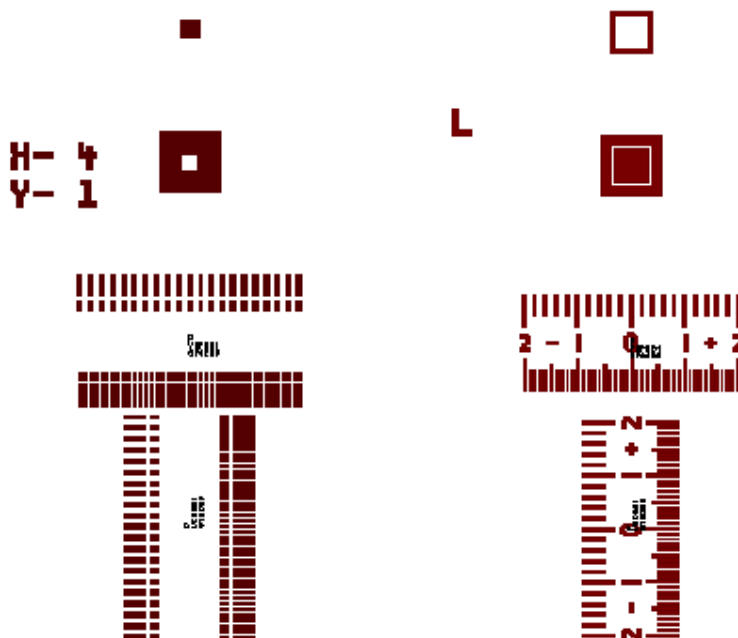


Figure 6: Test structures for 5x and 1x mix-and-match reticles.

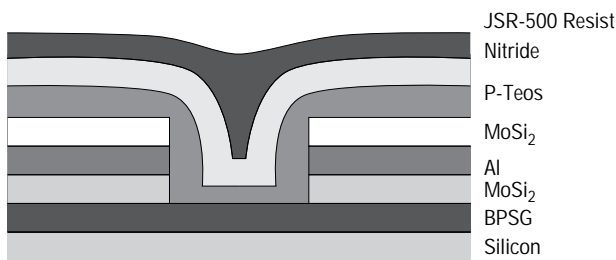
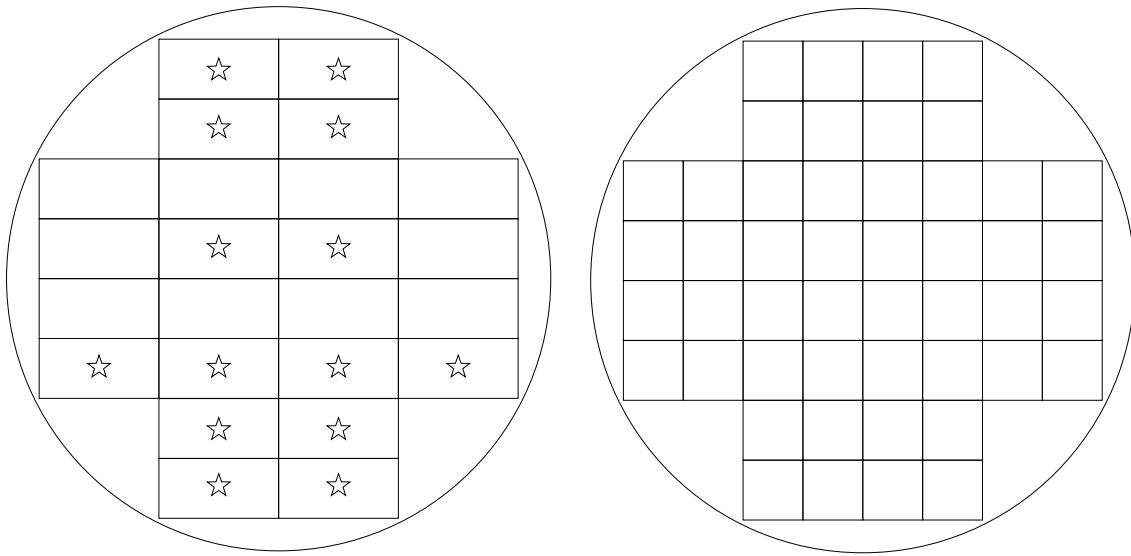


Figure 7: Cross sectional view of the composite film stack for the mix-and-match lithography wafers.



Ultratech 2244i

Canon 5x stepper

Figure 8: Wafer layouts for the Ultratech 2244i and the Canon Steppers.

Term	Corrected	Noncorrected
x mean (nm)	4	36
x sigma (nm)	43	62
y mean (nm)	12	-37
y sigma (nm)	33	47

Table 3: Summary of mix-and-match overlay errors for both the corrected and noncorrected reticles.

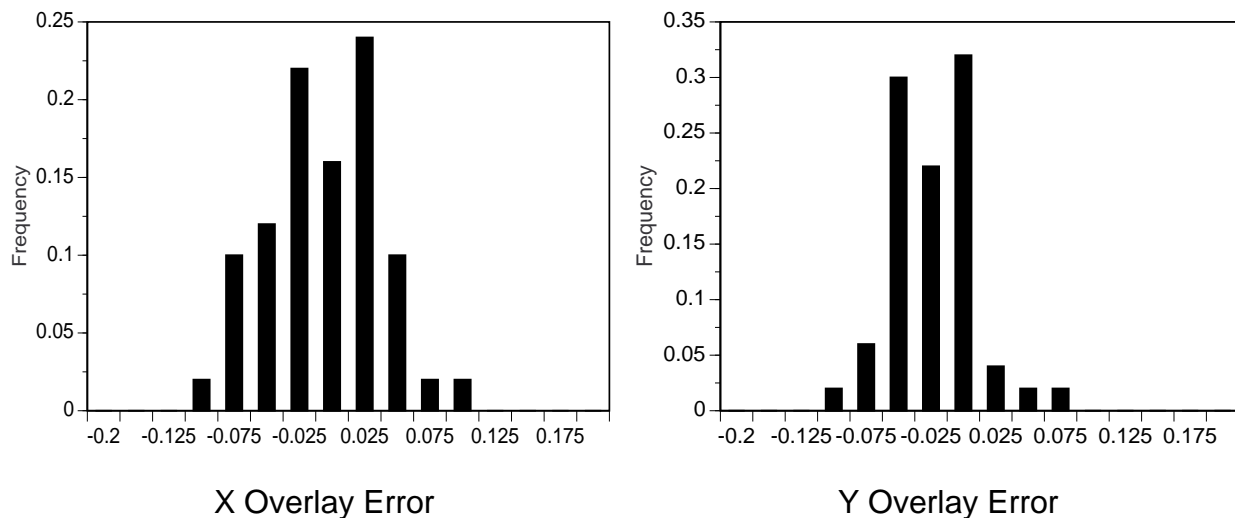


Figure 9: Histograms of x and y mix-and-match overlay errors for the corrected reticle.

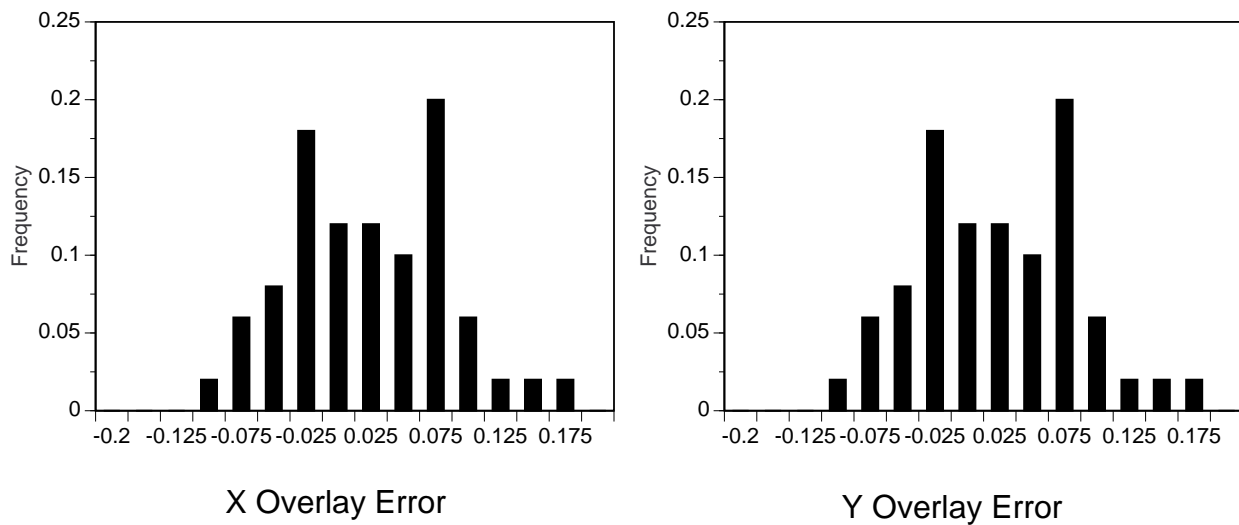


Figure 10: Histogram of x and y mix-and-match overlay errors for the noncorrected reticle.